Biophysical Reports

REPORT

Sub-quantal release is not dominant during prolonged depolarization in adrenal chromaffin cells

Lisi Wei,[1] Xin Wang,[1] Min Sun,[1] Wonchul Shin,[1] Kevin D. Gillis,[2] and Ling-Gang Wu[1,*]

[1]National Institute of Neurological Disorders and Stroke, 35 Convent Dr., Bldg. 35, Bethesda, MD 20892, USA and [2]Department of Chemical and Biomedical Engineering, University of Missouri, Columbia, MO 65201, USA

ABSTRACT Exocytosis, which mediates important functions like synaptic transmission and stress responses, has been postulated to release all transmitter molecules in the vesicle in the "all-or-none" quantal hypothesis. Challenging this hypothesis, amperometric current recordings of catecholamine release propose that sub-quantal or partial transmitter release is dominant in various cell types, particularly chromaffin cells. The sub-quantal hypothesis predicts that fusion pore closure (kiss-and-run fusion), the cause of sub-quantal release, is dominant, and blocking pore closure increases quantal size. We tested these predictions by imaging fusion pore closure and amperometric recording of catecholamine release in chromaffin cells during high potassium application, the most-used stimulation protocol for sub-quantal release study. We found that fusion pore closure is not predominant, and inhibition of the fusion pore closure does not increase the quantal size calculated from the amperometric current charge when a sufficiently long integration time is used. These results suggest that sub-quantal release is not prevalent during high potassium application in adrenal chromaffin cells.

WHY IT MATTERS Challenging the "all-or-none" quantal hypothesis established in the 1950s, recent studies suggest that sub-quantal release, the release of a fraction of transmitter molecules in a vesicle, is prevalent in secretory cells, particularly neuroendocrine cells. However, the release is estimated by integrating amperometric currents reflecting catecholamine release for only ~50 ms, which may underestimate prolonged releases. Here, we re-examined this sub-quantal release proposal in adrenal chromaffin cells by integrating amperometric current charge for 500 ms and by determining whether fusion pore closure, the kiss-and-run fusion that may cause partial release, is dominant. We found that sub-quantal release is not predominant during prolonged depolarization induced by high-potassium stimulation. More direct evidence is still needed to establish sub-quantal release as a major fusion mode in the future.

INTRODUCTION

Vesicle fusion from secretory cells releases neurotransmitters, peptides, and hormones to mediate many important functions, such as synaptic transmission essential for brain functions, stress responses, immune responses, and regulation of the blood glucose level (1–4). Vesicle fusion has been thought to release the entire vesicular content ever since Katz and his colleagues proposed the "all-or-none" quantal theory in the 1950s (3,5–7). Early amperometric recordings of vesicular catecholamine release in adrenal chromaffin or PC12 cells reveals small and slow amperometric currents (often called stand-alone foot signals) in a minor fraction of fusion events, raising the possibility of sub-quantal or partial release, the release of only a fraction of transmitter molecules in a vesicle (8–12). Consistently, imaging in chromaffin cells and PC12 cells suggests that large vesicular lumen proteins, such as neuropeptide Y attached with a fluorescent protein, may not be released upon fusion pore opening, albeit at a low frequency (13,14). Fusion pore conductance measurement of endocrine dense-core vesicles and synaptic clear-core vesicles revealed a small fusion pore that might limit transmitter release in a small fraction of fusion events, consistent with the sub-quantal release as an infrequent fusion mode (7,11,15).

In the last decade, electrochemical cytometry techniques have been developed to estimate the transmitter amount of a vesicle when the vesicle is absorbed and ruptured at the microelectrode in PC12

Submitted December 11, 2024, and accepted for publication May 2, 2025.

*Correspondence: wul@ninds.nih.gov

Wonchul Shin's present address is National Institute on Deafness and Communication Disorders, 35 Convent Dr., Bldg. 35, Bethesda, MD 20892, USA

Lisi Wei and Xin Wang contributed equally to this work.

Editor: Dong Li.

https://doi.org/10.1016/j.bpr.2025.100212

cells and adrenal chromaffin cells (16–18). Such an estimate is ∼70%–150% larger than the amount of released catecholamine during high potassium application, leading to the proposal that sub-quantal or partial release is predominant (18,19). Since the estimate is from two different conditions (vesicle rupture at the electrode versus vesicle fusion), it remains unclear whether the efficiency of electrochemical cytometry in capturing all released catecholamine molecules is the same. An estimate of ^{13}C-labeled dopamine with nano secondary ion mass spectrometry showed reduced vesicular dopamine after exocytosis, in line with the sub-quantal release hypothesis (20).

Many studies of dynamin, which is localized in the release site to constrict the fusion pore (14,21), use carbon electrodes to detect amperometric currents that reflect catecholamine release (22–24). Application of dynamin inhibitors, antibodies, or knockout of dynamin 1 increased the amperometric current charge by ∼50%–100% during high-potassium stimulation or repetitive firing, leading to the proposal that sub-quantal release is predominant during prolonged depolarization (22–24). However, in these studies, the amperometric current charge was calculated by integrating currents for only 50 ms or an unspecified time. Such an integration may miss the slow release. Indeed, many typical amperometric current traces published last longer than 50 ms (9,11,12,22–24), suggesting that a longer integration time is needed for accurate estimate of slow release.

Although many studies proposed the sub-quantal release as the predominant release mode during high potassium application, the key evidence for establishing this hypothesis, the kiss and run (fusion pore closure), the presumed cause of sub-quantal release, as the predominant fusion mode is missing. The hypothesis that sub-quantal release is predominant predicts that 1) kiss and run is predominant, and 2) inhibition of dynamin, which mediates fusion pore closure (14,21,25,26), should enhance the amperometric current charge even with a longer integration time. Here, we tested these predictions during high potassium application, the most-used stimulation condition to study sub-quantal release (13,17,18,20,23,24,27), in adrenal chromaffin cells. We used the imaging methods (14,21,25,26) to detect kiss and run and a microchip amperometric method (27–29) to detect catecholamine release. Our results suggest that sub-quantal release is not prevalent during prolonged depolarization.

MATERIALS AND METHODS

Bovine chromaffin cell culture

Chromaffin cells were isolated from bovine adrenal glands as previously reported (30). Briefly, after fat tissue was removed, adrenal glands were washed with Locke's solution (145 mM NaCl, 5.4 mM KCl, 2.2 mM Na_2HPO_4, 0.9 mM NaH_2PO_4, 5.6 mM glucose, and 10 mM HEPES, pH 7.3, adjusted with NaOH) and then digested with an enzyme mix that contains 1.5 mg/mL collagenase P, 0.325 mg/mL trypsin inhibitor, and 5 mg/mL bovine albumin serum dissolved in Locke's solution at 37°C for 20 min. After digestion, glands were cut longitudinally to expose soft digested medulla. Then, medulla was collected and minced in Locke's solution into small pieces to release chromaffin cells. Next, cell suspension was filtered through 80- to 100-μm nylon mesh and centrifuged at 520 rpm to collect the chromaffin cells pellet. Chromaffin cells were resuspended in pre-warmed DMEM low-glucose medium (GIBCO) supplemented with 10% fetal bovine serum (GIBCO) for experiments.

Buffer solution, plasmid and fluorescent dyes

Chromaffin cells were incubated in bath solution for amperometric recording or confocal imaging. Bath solution contains 150 mM NaCl, 5 mM KCl, 5 mM $CaCl_2$, 2 mM $MgCl_2$, 10 mM glucose, and 10 mM HEPES (pH 7.2). Exocytosis was induced by applying a high-potassium solution containing 85 mM NaCl, 70 mM KCl, 5 mM $CaCl_2$, 2 mM $MgCl_2$, 10 mM HEPES, and 10 mM glucose. Unless specified otherwise, all reagents were obtained from Sigma. Imaging of fusion pore closure involves using mNeonGreen attached to phospholipase C δPH domain (PH_G, overexpressed, binds to $PI(4,5)P_2$) to label the plasma membrane, and Atto 655 (A655, Sigma) to fill the fusing vesicle cavity (26). PH_G was created from PH-EGFP (from Dr. Tamas Balla) by replacing EGFP with mNeonGreen (Allele Biotechnology). FFN 511 (Abcam, Cambridge, United Kingdom) was loaded at 5–10 μM at 37°C for 10 min, and images were performed after washing out FFN 511 in the bath. A655 was included in the bath solution at 30 μM. Dynasore (80 μM, bath, 20–30 min) was from Millipore Sigma.

Electroporation and plating

PH_G was transfected via electroporation using Basic Primary Neurons Nucleofector Kit (Lonza) following the manufacturer's protocol and then plated onto poly-L-lysine and laminin-coated glass coverslips. Cells were incubated at 37°C with 9% CO_2 for 2–3 days before use.

Confocal imaging and analysis

Confocal imaging of PH_G, A655, and FFN511 was performed with a Leica TCS SP8 inverted confocal microscope (Leica, Germany) equipped with a 100× 1.4 NA HC PL APO CS2 oil-immersion objective. PH_G, A655, and FFN511 were excited by a tunable white light laser at 505 nm (laser power ∼1–4 mW), 633 nm (laser power ∼12–15 mW), and 442 nm (laser power ∼2–4 mW), respectively, and their fluorescence signals were collected with Leica HyD detectors at 515–575, 650–740, and 465–510 nm, respectively. Confocal imaging was performed at the *xy* plane with a fixed *z*-axis focal plane ∼100–200 nm above the cell-bottom membrane; images were collected every 40–120 ms at 40–60 nm per pixel. Detection of fusion pore closure and fusion modes are described in the results section.

Amperometric recording and analysis

The methods were described previously (27–29). Cultured chromaffin cells were detached from 30-mm dishes by vigorous washing with bath solution. After centrifuging twice at 120 rpm for 2 min and discarding the supernatant, the cells were

resuspended in 1 mL of bath solution resulting in a typical cell density of $\sim 2 \times 10^6$ cells/mL. 100 μL of cell solution was loaded into the microchip device and gently shaken several times to help the cells settle into the SU-8 microwells under gravity. After waiting for 15–20 min to allow the cell to settle, the device was washed with bath solution twice to remove unattached cells. Exocytosis was induced by applying a high-potassium solution.

The microchip devices with accompanying potentiostats and data-collection software were from ExoCytronics (27–29). These consist of a glass coverslip patterned with the transparent electrode material indium tin oxide (31). Inactive areas of indium tin oxide are insulated with a 14-μm-thick film of SU8. Working electrodes are defined as photolithographically patterned openings in the SU8 that are 20 μm in diameter. These microwells serve to trap a single cell in each well-electrode and enable recording of amperometric currents reflecting exocytosis from vesicles on the bottom surface of the cell. Each microchip device contained 16 or 32 electrodes and was connected to a custom 16-channel potentiostat. After an Ag|AgCl reference electrode was inserted into the bath and connected to the ground, power was supplied to the chip along with the clock signals. Initially, the potentiostat outputs were saturated due to the capacitive currents charging the electrode capacitance to 600 mV, followed by a slow decay to a minimal stable baseline current within 1 min (27–29). Amperometric recordings were sampled at 5-kHz sampling frequency and low-pass filtered at 500 Hz. All experiments were performed at room temperature unless otherwise indicated. IGOR PRO software (Wavemetrics) was used for offline data analysis, including spike amplitude, halfwidth, and charges. The data were first digitally low-pass filtered by 5-s binomial smoothing in IGOR PRO and then manually inspected, and overlapping or anomalous spikes (rise time more than 50 ms) were discarded.

Statistical tests

Data were expressed as mean + SE. The statistical test is the unpaired *t*-test, and ANOVA and Games-Howell *post hoc* test was used for multiple group comparison (32,33).

RESULTS

Fusion pore closure is infrequent during prolonged depolarization

If sub-quantal release is dominant, the kiss and run should be prevalent. We tested this prediction by the imaging technique we developed to resolve fusion pore closure (14,21,25,26). This technique involves using mNeonGreen attached to phospholipase C δPH domain (PH_G, overexpressed, binds to $PI(4,5)P_2$) to label the plasma membrane and Atto 655 (A655, in bath) to fill the fusing vesicle cavity (Fig. 1 *A*) (26). At the confocal *xy* plane ~100–200 nm above the cell-bottom plasma membrane (Fig. 1 *A*, dotted line: *z*-axis focal plane), fusion spots were detected as a sudden appearance of PH_G spots or rings together with A655 spots at the same location (Figs. 1 *B* and S1), due to the diffusion of PH_G and A655 from the plasma membrane and the bath, respectively, to the fusion-generated Ω-profiles (Fig. 1 *B–E*). Diffusion of these two fluorescent labels was directly observed with stimulated emission depletion (STED) imaging at the *xz* plane (14,21,26). When the vesicle lumen was loaded with fluorescent neuropeptide Y or a fluorescent false neurotransmitter FFN511, the sudden appearance of PH_G/A655 spots evoked by 1-s depolarization was accompanied by the release of neuropeptide Y or FFN511 at the same spot, confirming vesicle fusion in generating PH_G/A655 spots (14,26,34). This observation was verified during depolarization induced by 70 mM KCl (4 cells; Fig. S2 *A* and *B*).

With strong excitation of A655, imaging of the fusion-generated PH_G/A655 spots revealed three fusion modes: 1) close fusion (kiss and run), fusion-generated Ω-profile pore closure was detected as A655 fluorescence (F_{655}, strongly excited) dimming due to pore closure that prevented bath fluorescent A655 from exchanging with bleached A655, whereas PH_G fluorescence (F_{PH}, weakly excited) sustained or decayed with a delay (Fig. 1 *C*) (14,21,25,26); 2) stay fusion, a sustained fusion-generated Ω profile was detected as persistent PH_G/A655 spots with sustained F_{655} and F_{PH} (Fig. 1 *D*); and 3) shrink-fusion, fusion-generated Ω-profile shrinking was detected as parallel decreases of F_{655} and F_{PH} accompanied by the spot-size decrease (Fig. 1 *E*) (14,25,35). These fusion modes were directly observed and thus verified with STED imaging at the *xz*-plane, at which the vesicular Ω-shape can be clearly resolved (14,35). For the close fusion detected with PH_G/A655 imaging, bath application of an acid solution cannot quench the pH-sensitive VAMP2-EGFP or VAMP2-pHluorin overexpressed at the same fusion spot, confirming that the detected fusion pore closure is impermeable to H^+ or OH^-, the smallest molecules, and thus is functionally closed (21,25,26). Furthermore, the PH_G/A655-imaging-detected close fusion was blocked by dynamin inhibitor Dynasore, dynamin dominant-negative mutant dynamin 1-K44A, or dynamin 1/2 knockdown, suggesting that fusion pore closure is mediated by dynamin (21,25,26,36). These various dynamin-inhibition approaches blocked close fusion and thus converted close fusion into stay and shrink fusion (21,25,26). Although the above results regarding dynamin-mediated fusion pore closure were obtained with 1-s depolarization, dynamin is expected to mediate fusion pore closure during prolonged depolarization induced by high potassium application.

During 70 mM KCl application, 5% ± 2% of fusion events (total fusion events, 335 from 14 cells) was close fusion, whereas the remaining overwhelming majority was either stay- (77% ± 5% of fusion events) or shrink-fusion (18% ± 4% of fusion events) events (Fig. 1 *F*). This observation indicates that close fusion or kiss and run, the presumed cause for sub-quantal release, is rather infrequent during prolonged

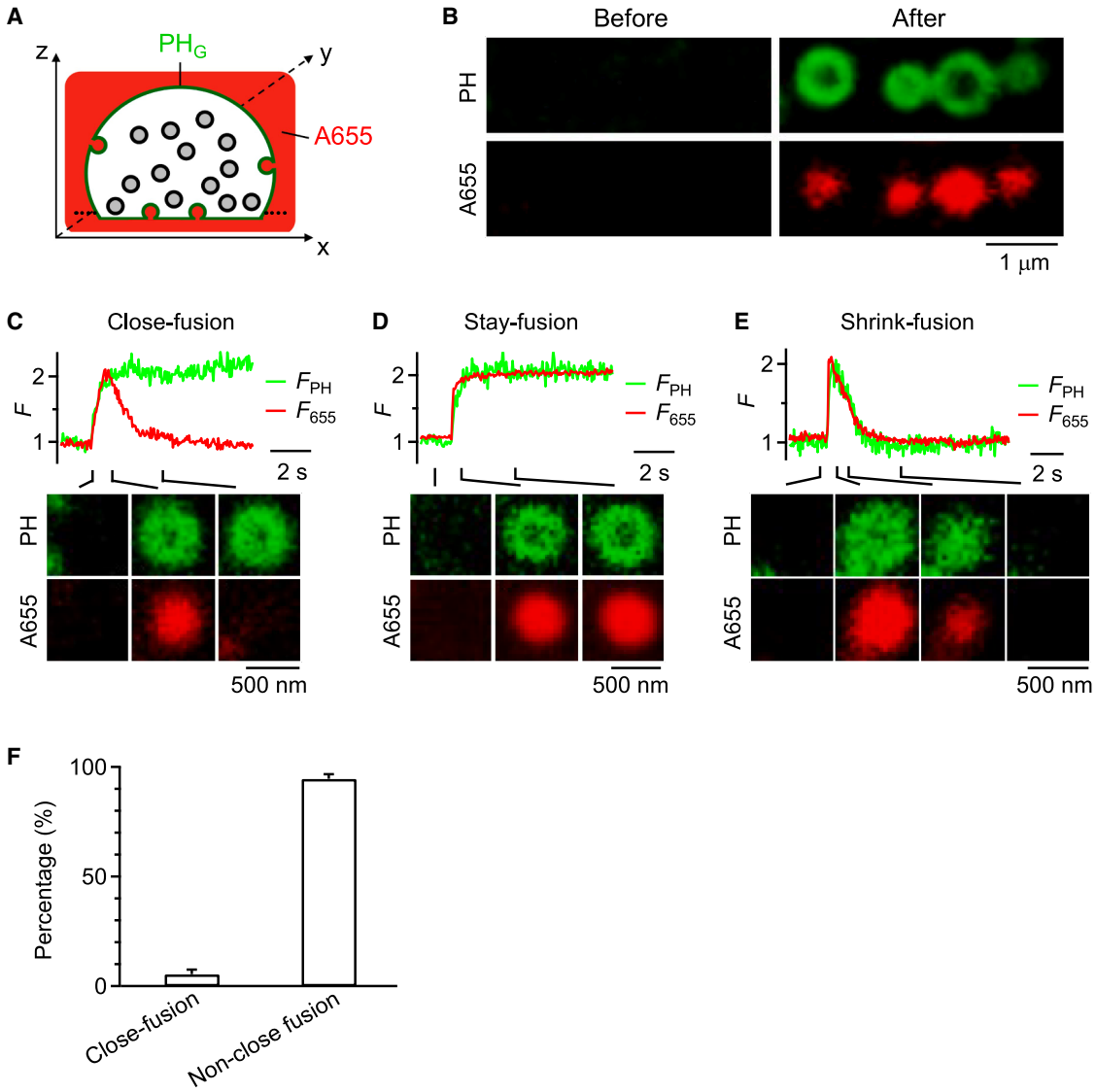

FIGURE 1 Fusion pore closure is infrequent during high potassium application. (*A*) Setup drawing: the cell plasma membrane is labeled with PH_G (*green*, overexpressed), and the bath solution includes A655 (*red*) for the detection of fusion spots. The microscopic *x*, *y*, and *z* axes are also labeled. The dotted line indicates the *z*-axis focal plane. (*B*) Sampled PH_G and A655 images for four fusion events before and after fusion during high potassium application. The time interval between these two images is 14.4 s. (*C–E*) Fluorescence, F, of PH_G (F_{PH}, green) and A655 (F_{655}, red), and sampled confocal images showing close fusion (*C*), stay fusion (*D*), or shrink-fusion (*E*) recorded during high-potassium (70 mM) application. F_{PH} and F_{655} are normalized to the baseline before fusion. (*F*) The percentage (mean + SE) of close and nonclose (stay- and shrink-fusion) fusion events during high potassium application (335 fusion events from 14 cells).

depolarization, questioning the hypothesis that sub-quantal release is the predominant fusion mode.

Dynasore increases the amperometric current amplitude, but is not charge integrated for 500 ms during prolonged depolarization

We tested whether inhibition of dynamin, which mediates fusion pore closure in chromaffin cells (14,21,25,26), enhances the amperometric current charge, a prediction if the sub-quantal release is predominant. Primary cultured bovine adrenal chromaffin cells were isolated from culture dishes and loaded into a microchip device for cells to settle into the microwells equipped with well-electrode microchips that oxidize catecholamine, generating amperometric currents to reflect catecholamine release (27–29). A solution containing 70 mM KCl was applied to cells to induce depolarization and catecholamine secretion (Fig. 2 *A–D*). Catecholamine release from single-vesicle fusion was detected as amperometric spikes from the microchip (Fig. 2 *A* and *B*). In control, the spike amplitude ranged from 0.4 to 109.0 pA, and the spike halfwidth time (the interval

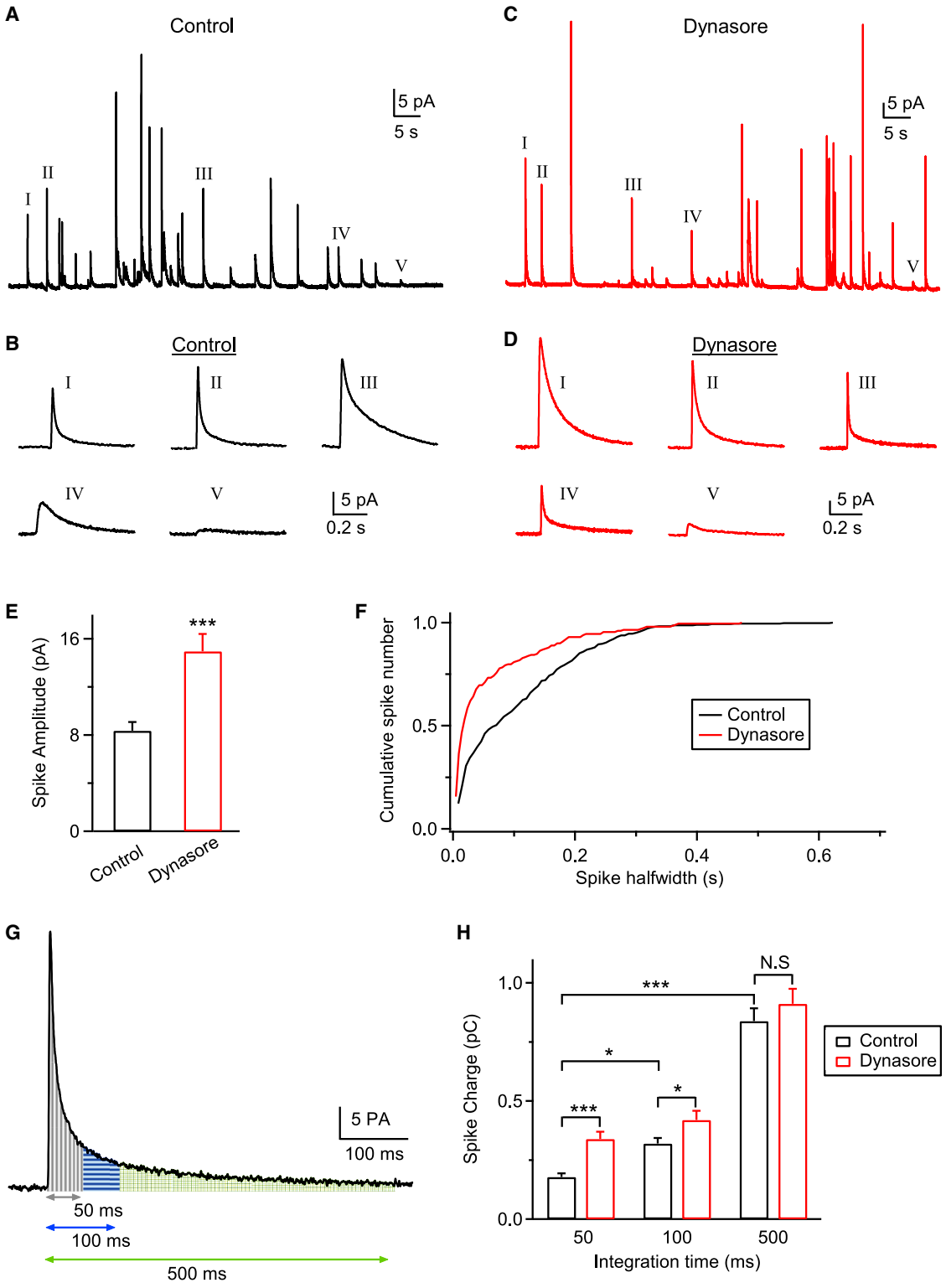

FIGURE 2 A dynamin inhibitor Dynasore increases spike amplitude, and reduces spike halfwidth, but does not affect spike charge integrated for 500 ms. (*A*) Sampled amperometric recordings during application of a high-potassium (70 mM) solution in the control condition without Dynasore treatment. (*B*) Five amperometric spikes taken from (*A*) (I–V) are enlarged. (*C* and *D*) Similar to (A) and (B), respectively, except that the cell was pre-incubated with 80 μM Dynasore in the bath solution for ~30 min. (*E*) The amperometric spike amplitude (mean + SE) during high potassium application in the absence (control, 48 cells) or presence (37 cells) of 80 μM Dynasore. ***$p < 0.001$, unpaired *t*-test. (*F*) Cumulative amperometric spike number plotted versus the spike halfwidth in the absence (control, 48 cells) or presence (37 cells) of

(legend continued on next page)

where the current exceeds 50% of the peak value) ranged from 5 to 626 ms (Fig. 2 *A*, *B*, *E*, and *F*). These values were in the same order as previous reports (27–29). The spike halfwidth histogram could be fitted with two Gaussian functions, centered at 20 ms (halfwidth = 44 ms, height = 0.16) and 120 ms (halfwidth = 200 ms, height = 0.03; Fig. S3 *A*), consistent with two populations of vesicles with different synaptotagmin isoforms and release kinetics (fast and slow) (37).

To determine whether inhibition of dynamin increases the quantal size during high potassium application as recently proposed (24), we used Dynasore, a dynamin inhibitor, to inhibit fusion pore constriction and closure. Dynasore inhibits dynamin specifically in chromaffin cells because, in this cell type, a series of studies repeatedly showed that, similar to dynamin 1/2 knockdown or overexpression of dynamin 1 K44A mutant, Dynasore inhibits fusion pore constriction and closure that antagonizes pore expansion, resulting in the speeding up of fusion pore expansion and block of fusion pore closure (14,21,25). In the presence of Dynasore (Fig. 2 *C* and *D*), the spike amplitude was substantially (∼78%) larger than the control (Figs. 2 *E* and S4 *A* and *B*); spike halfwidth distribution, including the two components identified in control, was significantly shifted to the left (Figs. 2 *F* and S3). These results are consistent with the reported increase of the amperometric spike amplitude in the absence of dynamin 1 (24) and the reported speeding up of fusion pore expansion as well as the block of fusion pore closure by Dynasore, dynamin 1/2 knockdown, or dynamin 1 K44A overexpression (14,21,25).

When the quantal size was quantified by integrating the amperometric spike for 50 ms as previously done (Fig. 2 *G*) (24), Dynasore substantially increased the quantal size by ∼88% (Fig. 2 *H*), consistent with the previous report that dynamin 1 knockout increased the spike amplitude by ∼50% (24). However, a substantial fraction of spikes showed spike halfwidth of more than 50 ms (Figs. 2 *F* and *G*), indicating that 50-ms integration is insufficient to account for these slow releases. Indeed, when the integration time was increased to 100 and 500 ms, the resulting charge was increased substantially (Fig. 2 *H*). With 100-ms integration time, Dynasore still increased the charge but to a smaller extent (∼31%; Fig. 2 *H*); with 500-ms integration time, Dynasore did not significantly increase the quantal size (Figs. 2 *H* and S4 *C* and *D*). These results suggest that inhibition of dynamin speeds up the release time course but does not affect the quantal size when slow release is taken into account with a longer integration time. Together with the PH_G/A655 confocal imaging, our data argue against sub-quantal release as the predominant fusion mode.

Dynasore has been shown to inhibit fluid-phase endocytosis in fibroblasts deficient of dynamin 1, 2, and 3 (38). For two reasons, this nonspecific effect is unlikely to account for our observation that Dynasore increased the spike amplitude but shortened the halfwidth. First, to our knowledge, the fluid-phase endocytosis is not related to the fusion pore dynamics studied here. Second, numerous studies showed that Dynasore mimics dynamin (isoform 1 and 2) knockdown or overexpression of dynamin 1 K44A (dominant negative) in inhibiting fusion and fission pore constriction and closure and diverse endocytic modes, including slow, fast, ultrafast, and overshoot endocytosis in chromaffin cells, suggesting that Dynasore inhibits dynamin-mediated fusion pore constriction and closure (14,21,25,36). Given that dynamin-mediated fusion pore constriction/closure competes with fusion pore expansion to determine the fusion pore dynamics in chromaffin cells (14), inhibition of dynamin-mediated fusion pore constriction/closure by Dynasore allows for faster fusion pore expansion and thus faster release, explaining Dynasore's effect in shortening the spike halfwidth but increasing the spike amplitude.

DISCUSSION

In bovine adrenal chromaffin cells, we established an *xy*-plane imaging technique to resolve fusion pore closure by using PH_G/A655 dyes combined with confocal and STED microscopy. In the current study, we applied high potassium to stimulate the vesicular fusion in chromaffin cells to measure the fusion pore closure. Contrary to previous reports that demonstrate sub-quantal release is predominant during high potassium application, we revealed only ∼5% close fusion (or kiss and run) (Fig. 1), the presumed cause of sub-quantal release, which is too small to support sub-quantal release as the predominant fusion mode (18,24). Besides, not all kiss-and-run events can produce sub-quantal release, because kiss-and-run fusions may release vesicular contents

80 μM Dynasore (maximal spike number is normalized to 1). (*G*) A sampled amperometric spike with the charge integrated for 50, 100, and 500 ms shown in different colors to show different quantal sizes resulting from the use of different integration times. (*H*) The amperometric spike charge (mean + SE) integrated for 50, 100, and 500 ms in the absence (control, 48 cells) or presence (37 cells) of 80 μM Dynasore. *p < 0.05; ***p < 0.001; N.S, p = 0.36 (ANOVA and Games-Howell *post hoc* test for multiple group comparison).

as fast as the non-kiss-and-run fusions in chromaffin cells (14) and may have fusion pores as large as non-kiss-and-run fusion as synapses (15). Further, we recorded amperometric spikes reflecting single-vesicle fusions evoked by prolonged depolarization during high potassium application (Fig. 2). We found that Dynasore, which has been shown to inhibit dynamin functions in chromaffin cells (14,21,25), increased the amperometric spike amplitude and reduced the spike halfwidth (Fig. 2). These results suggest that Dynasore accelerates the release time course, consistent with Dynasore's effect in blocking fusion pore constriction that antagonizes pore expansion, therefore resulting in faster fusion pore expansion (14,21).

Dynasore increased not only the amperometric spike amplitude but also the charge integrated for 50 ms (Fig. 2). This result is consistent with a recent study (24) that proposed prevalent sub-quantal release based on the observed increase of amperometric spike amplitude and charge integrated for 50 ms by dynamin 1 knockout. However, a substantial fraction of amperometric spikes' halfwidth was longer than 50 ms (Fig. 2), suggesting that integration of only 50 ms may significantly underestimate catecholamine release. Consistent with our observation, many sample amperometric current recordings in many published papers showed amperometric currents lasting longer than 50 ms (9,11,12,22–24). With an integration time of 500 ms, the charge was much larger, and Dynasore no longer increased the charge that takes slow release into account (Fig. 2), suggesting that sub-quantal release is not prevalent during high-potassium prolonged depolarization.

Although nonspecific effects of Dynasore have been reported (38), it should not affect our conclusion that the block of the fusion pore closure by Dynasore does not increase the quantal size in the present work. Furthermore, in chromaffin cells, Dynasore mimics dynamin 1/2 knockdown or overexpression of dynamin K44A (dominant-negative mutant) in blocking fusion pore closure, inhibiting preformed Ω-profiles' pore closure, and facilitating fusion pore expansion (14,21,25,26). These effects readily explain the effect of Dynasore in shortening the spike halfwidth and increasing the spike amplitude as observed in the present work (Fig. 2).

Although our results challenge the hypothesis that sub-quantal release is predominant, our data do not exclude the possibility that sub-quantal release of catecholamine exists but in a minority of events below our detection level. Our conclusion is limited to the prolonged depolarization during high potassium application, in which the prevalent sub-quantal release hypothesis was proposed in most recording conditions (13,17,18,20,23,24,27).

ACKNOWLEDGMENTS

This work was supported by NINDS Intramural Research Program (ZIA NS003009-15 and ZIA NS003105-10 to L.G.W.).

AUTHOR CONTRIBUTIONS

L.W., X.W., and M.S. performed experiments. W.S. and K.D.G. assisted on microchip experiments. X.W., L.W., and L.G.W. wrote the manuscript with help from all authors. L.G.W. designed experiments and supervised the project.

DECLARATION OF INTERESTS

K.D.G. has an equity interest in ExoCytronics, which develops electrochemical electrode devices and instruments for amperometric measurement of exocytosis.

SUPPORTING MATERIAL

Supporting material can be found online at https://doi.org/10.1016/j.bpr.2025.100212.

REFERENCES

1. Kasai, H., N. Takahashi, and H. Tokumaru. 2012. Distinct initial SNARE configurations underlying the diversity of exocytosis. *Physiol. Rev.* 92:1915–1964. https://doi.org/10.1152/physrev.00007.2012.
2. Rorsman, P., and M. Braun. 2013. Regulation of insulin secretion in human pancreatic islets. *Annu. Rev. Physiol.* 75:155–179. https://doi.org/10.1146/annurev-physiol-030212-183754.
3. Wu, L. G., E. Hamid, …, H. C. Chiang. 2014. Exocytosis and endocytosis: modes, functions, and coupling mechanisms. *Annu. Rev. Physiol.* 76:301–331. https://doi.org/10.1146/annurev-physiol-021113-170305.
4. van den Pol, A. N. 2012. Neuropeptide transmission in brain circuits. *Neuron.* 76:98–115. https://doi.org/10.1016/j.neuron.2012.09.014.
5. Fatt, P., and B. Katz. 1952. Spontaneous subthreshold activity at motor nerve endings. *J. Physiol.* 117:109–128.
6. Del Castillo, J., and B. Katz. 1954. Quantal components of the end-plate potential. *J. Physiol.* 124:560–573. https://doi.org/10.1113/jphysiol.1954.sp005129.
7. Sharma, S., and M. Lindau. 2018. The fusion pore, 60 years after the first cartoon. *FEBS Lett.* 592:3542–3562. https://doi.org/10.1002/1873-3468.13160.
8. Wightman, R. M., J. A. Jankowski, …, O. H. Viveros. 1991. Temporally resolved catecholamine spikes correspond to single vesicle release from individual chromaffin cells. *Proc. Natl. Acad. Sci. USA.* 88:10754–10758.
9. Chow, R. H., L. von Rüden, and E. Neher. 1992. Delay in vesicle fusion revealed by electrochemical monitoring of single secretory events in adrenal chromaffin cells. *Nature.* 356:60–63.
10. Alvarez de Toledo, G., R. Fernández-Chacón, and J. M. Fernández. 1993. Release of secretory products during transient vesicle fusion. *Nature.* 363:554–558.
11. Albillos, A., G. Dernick, …, M. Lindau. 1997. The exocytotic event in chromaffin cells revealed by patch amperometry. *Nature.* 389:509–512. https://pubmed.ncbi.nlm.nih.gov/9333242.
12. Zhou, Z., S. Misler, and R. H. Chow. 1996. Rapid fluctuations in transmitter release from single vesicles in bovine adrenal

chromaffin cells. *Biophys. J.* 70:1543–1552. https://doi.org/10.1016/s0006-3495(96)79718-7.

13. Taraska, J. W., D. Perrais, …, W. Almers. 2003. Secretory granules are recaptured largely intact after stimulated exocytosis in cultured endocrine cells. *Proc. Natl. Acad. Sci. USA.* 100:2070–2075. http://www.ncbi.nlm.nih.gov/pubmed/12538853.
14. Shin, W., L. Ge, …, L. G. Wu. 2018. Visualization of Membrane Pore in Live Cells Reveals a Dynamic-Pore Theory Governing Fusion and Endocytosis. *Cell.* 173:934–945.e12. https://doi.org/10.1016/j.cell.2018.02.062.
15. He, L., X. S. Wu, …, L. G. Wu. 2006. Two modes of fusion pore opening revealed by cell-attached recordings at a synapse. *Nature.* 444:102–105. http://www.ncbi.nlm.nih.gov/pubmed/17065984.
16. Dunevall, J., H. Fathali, …, A. G. Ewing. 2015. Characterizing the catecholamine content of single mammalian vesicles by collision-adsorption events at an electrode. *J. Am. Chem. Soc.* 137:4344–4346. https://doi.org/10.1021/ja512972f.
17. Li, X., S. Majdi, …, A. G. Ewing. 2015. Quantitative measurement of transmitters in individual vesicles in the cytoplasm of single cells with nanotip electrodes. *Angew. Chem. Int. Ed. Engl.* 54:11978–11982. https://doi.org/10.1002/anie.201504839.
18. Wang, Y., and A. Ewing. 2021. Electrochemical Quantification of Neurotransmitters in Single Live Cell Vesicles Shows Exocytosis is Predominantly Partial. *Chembiochem.* 22:807–813. https://doi.org/10.1002/cbic.202000622.
19. Borges, R., C. Gu, …, A. G. Ewing. 2023. The dynamic nature of exocytosis from large secretory vesicles. A view from electrochemistry and imaging. *Cell Calcium.* 110:102699. https://doi.org/10.1016/j.ceca.2023.102699.
20. Nguyen, T. D. K., L. Mellander, …, A. G. Ewing. 2022. Visualization of Partial Exocytotic Content Release and Chemical Transport into Nanovesicles in Cells. *ACS Nano.* 16:4831–4842. https://doi.org/10.1021/acsnano.2c00344.
21. Zhao, W. D., E. Hamid, …, L. G. Wu. 2016. Hemi-fused structure mediates and controls fusion and fission in live cells. *Nature.* 534:548–552. https://doi.org/10.1038/nature18598.
22. Elhamdani, A., H. C. Palfrey, and C. R. Artalejo. 2001. Quantal size is dependent on stimulation frequency and calcium entry in calf chromaffin cells. *Neuron.* 31:819–830.
23. Gonzalez-Jamett, A. M., X. Baez-Matus, …, A. M. Cardenas. 2010. The association of dynamin with synaptophysin regulates quantal size and duration of exocytotic events in chromaffin cells. *J. Neurosci.* 30:10683–10691. https://doi.org/10.1523/JNEUROSCI.5210-09.2010.
24. Wu, Q., Q. Zhang, …, Z. Zhou. 2019. Dynamin 1 Restrains Vesicular Release to a Subquantal Mode In Mammalian Adrenal Chromaffin Cells. *J. Neurosci.* 39:199–211. https://doi.org/10.1523/JNEUROSCI.1255-18.2018.
25. Chiang, H. C., W. Shin, …, L. G. Wu. 2014. Post-fusion structural changes and their roles in exocytosis and endocytosis of dense-core vesicles. *Nat. Commun.* 5:3356. https://doi.org/10.1038/ncomms4356.
26. Shin, W., L. Wei, …, L. G. Wu. 2021. Preformed Omega-profile closure and kiss-and-run mediate endocytosis and diverse endocytic modes in neuroendocrine chromaffin cells. *Neuron.* 109:3119–3134.e5. https://doi.org/10.1016/j.neuron.2021.07.019.
27. Liu, X., S. Barizuddin, …, K. D. Gillis. 2011. Microwell device for targeting single cells to electrochemical microelectrodes for high-throughput amperometric detection of quantal exocytosis. *Anal. Chem.* 83:2445–2451. https://doi.org/10.1021/ac1033616.
28. Ghosh, J., X. Liu, and K. D. Gillis. 2013. Electroporation followed by electrochemical measurement of quantal transmitter release from single cells using a patterned microelectrode. *Lab Chip.* 13:2083–2090. https://doi.org/10.1039/c3lc41324a.
29. Gillis, K. D., X. A. Liu, …, V. Carabelli. 2018. Electrochemical measurement of quantal exocytosis using microchips. *Pflugers Arch.* 470:97–112. https://doi.org/10.1007/s00424-017-2063-2.
30. Guo, X., S. Han, …, L. G. Wu. 2022. Real-time visualization of exo- and endocytosis membrane dynamics with confocal and super-resolution microscopy. *STAR Protoc.* 3:101404. https://doi.org/10.1016/j.xpro.2022.101404.
31. Sun, X., and K. D. Gillis. 2006. On-chip amperometric measurement of quantal catecholamine release using transparent indium tin oxide electrodes. *Anal. Chem.* 78:2521–2525. https://doi.org/10.1021/ac052037d.
32. Toothaker, L. E. 1993. Multiple comparison procedures. Sage, Newbury Park, CA.
33. Ruxton, G. D., and G. Beauchamp. 2008. Time for some a priori thinking about post hoc testing. *Behav. Ecol.* 19:690–693. https://doi.org/10.1093/beheco/arn020.
34. Ge, L., W. Shin, …, L. G. Wu. 2022. Sequential compound fusion and kiss-and-run mediate exo- and endocytosis in excitable cells. *Sci. Adv.* 8:eabm6049. https://doi.org/10.1126/sciadv.abm6049.
35. Shin, W., G. Arpino, …, L. G. Wu. 2020. Vesicle Shrinking and Enlargement Play Opposing Roles in the Release of Exocytotic Contents. *Cell Rep.* 30:421–431.e7. https://doi.org/10.1016/j.celrep.2019.12.044.
36. Shin, W., B. Zucker, …, L. G. Wu. 2022. Molecular mechanics underlying flat-to-round membrane budding in live secretory cells. *Nat. Commun.* 13:3697. https://doi.org/10.1038/s41467-022-31286-4.
37. Bendahmane, M., A. Morales, …, A. Anantharam. 2020. Synaptotagmin-7 enhances calcium-sensing of chromaffin cell granules and slows discharge of granule cargos. *J. Neurochem.* 154:598–617. https://doi.org/10.1111/jnc.14986.
38. Park, R. J., H. Shen, …, P. De Camilli. 2013. Dynamin triple knockout cells reveal off target effects of commonly used dynamin inhibitors. *J. Cell Sci.* 126:5305–5312. https://doi.org/10.1242/jcs.138578.